A Cumulus Parameterization Based on the Generalized Convective Available Potential Energy

JUNYI WANG AND DAVID A. RANDALL

Department of Atmospheric Science, Colorado State University, Fort Collins, Colorado

(Manuscript received 13 February 1995, in final form 11 September 1995)

ABSTRACT

This paper reports tests of a cumulus parameterization in which the reference state associated with the generalized convective available potential energy (GCAPE) is chosen as the end-state of the convective adjustment. The GCAPE is defined as the enthalpy difference between the given state and the reference state and represents the total potential energy available for conversion into convective kinetic energy in a given sounding. The reference state is the unique state in which the system enthalpy is minimized; it is also a statically neutral or stable state. By assuming that convection drives the atmosphere from the given state toward the reference state, we can use Nitta's diagnostic method to determine the cloudbase mass flux in a prognostic model. The adjustment timescale is finite and varies, depending on the intensity of the large-scale forcing, so this is a "relaxed" scheme. The effects of detrainment are parameterized in a very simple way. After the cloudbase mass flux has been obtained, Nitta's method and Johnson's simple downdraft model are used to determine the feedback of cumulus convection on the large-scale temperature and moisture fields. We have performed a semiprognostic test of the new adjustment scheme using the GATE Phase III data. The results are in fair agreement with observations.

1. Introduction

It is well known that cumulus convection, especially deep and intense convection, is one of the major processes affecting the dynamics and energetics of large-scale atmospheric circulations. One of the important effects of cumulus convection on the large-scale thermodynamic structure is to release the convective instability so as to modify or "adjust" a conditionally unstable atmosphere toward a more stable state that can be called the equilibrium state. This is the basis of the various convective adjustment schemes. The key problems are specification of the equilibrium state and the criterion for activation of convection. These differ from scheme to scheme.

The simplest cumulus parameterizations are the moist convective adjustment (MCA) schemes (Manabe et al. 1965; Miyakoda et al. 1969; Krishnamurti and Moxim 1971; Kurihara 1973). In MCA, it is assumed that deep moist convection acts to restore the lapse rate to a saturated moist adiabat, which can be called the "equilibrium state." When the large-scale sounding becomes more unstable than the equilibrium state, and if sufficient moisture is available, the sounding is adjusted toward the equilibrium state. This stabilization is attributed to cumulus convection. The main limitations of MCA are that it does not simulate penetrative convection and that the equilibrium state is saturated and so not very realistic.

Arakawa and Schubert (1974) developed a sophisticated cumulus parameterization that includes many physical processes. It can be viewed as an adjustment scheme. In the Arakawa–Schubert (AS) parameterization, a spectrum of cloud types is considered, so that the effects of different cloud types can be seen explicitly. Also, the AS parameterization relates convective activity to the large-scale forcing, which involves horizontal and vertical advections, radiation, and the surface fluxes of sensible heat and moisture. In particular, the AS parameterization makes use of the assumption that the real atmosphere is in a quasi-equilibrium state, in which the rate of destabilization by large-scale processes and the rate of stabilization by cumulus convection almost balance each other. That is, the large-scale forcing produces convective clouds, and the clouds consume the instability generated by the large-scale forcing, so that the atmosphere stays close to an equilibrium state in which the conditional instability is weak or nonexistent. In this sense, the AS parameterization is an adjustment scheme.

According to the quasi-equilibrium hypothesis, the rate of instability increase due to large-scale processes is fully and immediately counteracted by convection so that the atmosphere does not become very unstable. The assumption of such a quasi-equilibrium means that the AS parameterization cannot predict the convective available potential energy (CAPE) stored in a weather

Corresponding author address: Dr. Junyi Wang, Center for Cloud, Chemistry and Climate, Scripps Institution of Oceanography, University of California at San Diego, La Jolla, CA 92093-0239.

system. Some "relaxed" schemes, in which the exact quasi-equilibrium assumption is not strictly enforced, have been developed to implement the AS parameterization (e.g., Moorthi and Suarez 1992; Randall and Pan 1993). These schemes adjust toward the equilibrium state over a finite timescale.

Betts (1986) and Betts and Miller (1986) presented a "relaxed" convective adjustment scheme in which, as in the other adjustment schemes, a conditionally unstable sounding is adjusted by convection toward an equilibrium state. They specified the equilibrium temperature sounding to follow a virtual moist adiabat at low levels and a pseudoadiabat at high levels. They specified the equilibrium moisture profile empirically, although in fact it may vary for different regions and synoptic situations. The feedbacks between cumulus clouds on the large-scale environment were not explicitly or "mechanistically" represented, for example, in terms of mass fluxes.

Since the fundamental physical basis of adjustment methods is that convection acts to release the convective instability (or conditional instability) so as to drive the atmosphere toward a neutral state, a measure of the conditional instability is a key ingredient of such schemes. The conventional methods of measuring conditional instability are not fully satisfactory, however: the effects of environmental return flow are neglected, and the level of origination of the lifted parcel must be assumed. The generalized convective available potential energy (GCAPE) of Randall and Wang (1992) overcomes these restrictions and therefore is a prior more accurate measure of the conditional instability. Based on Lorenz's (1978, 1979) concept of moist available energy (MAE) Randall and Wang (1992) defined the GCAPE as the "vertical component" of the MAE and used it as a measure of the conditional instability of an atmospheric column. The definition of the GCAPE makes a "reference state," which is the unique state in which the system's enthalpy is minimized; it is also a statically neutral or stable state. The GCAPE is the vertically integrated enthalpy difference between a given state and the corresponding reference state and represents the total potential energy available for convection in a given sounding.

In this paper, we propose an adjustment scheme based on the concept of GCAPE. This new parameterization combines some elements of the Arakawa–Schubert parameterization and the Betts–Miller parameterization and tries to correct some limitations of those two parameterizations. The reference state associated with the GCAPE is chosen as the end-state of the adjustment or the equilibrium state. This equilibrium state is determined by the given state so that it varies in space and time. We relax toward the equilibrium state (as in the Betts–Miller parameterization), so that no strict quasi-equilibrium between large-scale forcing and convection is imposed.

We are attracted to the idea of using the GCAPE reference state as the equilibrium state of the adjustment because the GCAPE reference state is completely general and is not based on a cloud model. We have to keep in mind, however, that the GCAPE reference state is reached by reversible adiabatic processes. Real convection involves crucially important irreversible processes such as precipitation and mixing. Obviously, a cumulus parameterization has to take these irreversible processes into account.

We take them into account by using a simple cloud model. This means that although we avoid the use of a cloud model in the definition of the equilibrium state, we do use one to determine the convective feedback.

One might argue that an ideal cumulus parameterization would avoid using any cloud model at all. This is the idea behind the Betts–Miller parameterization. It is also the idea behind the empirical cumulus parameterization developed by Liu (1995), who used the logical framework of the AS parameterization but employed both an empirical equilibrium state (in which an empirically defined measure of CAPE is small) and an empirical formulation for the feedback of the convection on the large-scale fields.

It seems desirable to avoid both empiricism and cloud models as far as possible. The present study aims to show that it is possible to use the concept of GCAPE to define the equilibrium state without using empiricism or cloud models, but we do resort to a cloud model to determine the convective feedback.

There is no contradiction between the use of the idealized reference state that is defined with respect to adiabatic reversible processes and the simultaneous use of a cloud model that includes irreversible processes such as mixing and precipitation. Our idea is that the convection "tries" to adjust to the reference state but that irreversible processes prevent this adjustment from being fully realized.

The incorporation of a cloud model inevitably and regrettably causes our parameterization to fall far short of the power and generality of Lorenz's MAE concept. For example, the cloud model does assume particular levels of origin for the updrafts and downdrafts.

As explained in detail later, we use the predicted (or observed) sounding and the corresponding GCAPE reference state, together with a relaxation timescale (discussed below), to determine the convective tendency of the moist static energy. This is not enough for a cumulus parameterization, however. In a prognostic model we need to know the tendencies of temperature and moisture separately. In order to find them, we introduce the cloud model mentioned above, the form of the diagnostic model of Nitta (1975), modified to in-

corporate the downdrafts of Johnson (1976).[1] The convective moist static energy tendency is used as input to the diagnostic model, which determines the corresponding tendencies of temperature and moisture and also yields the precipitation rate.

A second new aspect of our parameterization is that we relate the adjustment timescale to the large-scale forcing so that the intensity of cumulus convection is controlled by the large-scale forcing (as in the Arakawa–Schubert parameterization).

Section 2 explains how we adapt Nitta's (1975) diagnostic method to determine the cloudbase mass flux. Section 3 presents a way to determine the adjustment timescale. Section 4 describes the data used in this study. Section 5 presents the results of some preliminary tests. In section 6, we present a simple approach to include the effects of detrainment. Section 7 summarizes the results of semiprognostic tests of the proposed scheme, using data from the Global Atmosphere Research Program's Atlantic Tropical Experiment (GATE) Phase III. Brief comparisons of the proposed parameterization with the Betts–Miller parameterization and the Arakawa–Schubert parameterization and a concluding discussion are presented in section 8.

2. Closure assumption

Nitta (1975) designed a parameterization to determine the cloud-base mass flux from the large-scale moist static energy budget by using the cloud model of Arakawa and Schubert (1974). A brief description of Nitta's method is given in the appendix. Nitta's method can be used (e.g., Nitta 1975, Johnson 1976, Cheng 1989, Wu 1993) to obtain the cloudbase mass flux $m_B(\lambda)$ diagnostically when $(Q_1 - Q_2 - Q_R)$ is known from observations. Here Q_1 is the apparent heating source, Q_2 is the apparent moisture sink, and Q_R is the radiative heating rate (Yanai et al. 1973). The equation that is solved to determine the cloud base mass flux is (A6). The input is $(Q_1 - Q_2 - Q_R)$.

Before we can use Nitta's method in a cumulus parameterization, we must find a way to determine $(Q_1 - Q_2 - Q_R)$. As shown by Yanai et al. (1973),

$$Q_1 - Q_2 - Q_R = -\frac{\partial}{\partial p}\overline{(s' + Lq')\omega'} = -\frac{\partial}{\partial p}\overline{h'\omega'}. \tag{1}$$

Here s is the dry static energy, L is the latent heat of condensation, q is the water vapor mixing ratio, h is the moist static energy, and ω is the vertical p velocity. Horizontal large-scale averages are denoted by overbars, and deviations from these averages are denoted by primes. Thus, $(Q_1 - Q_2 - Q_R)$ represents the vertical convergence of the eddy transport of moist static energy, and of course this eddy transport is primarily due to moist convection. A typical distribution of moist static energy in the tropical troposphere has a minimum in the midtroposphere and maxima near the surface and the tropopause. The primary mechanism through which a cumulus ensemble affects the large-scale fields is by inducing subsidence between the clouds (Yanai et al. 1973; Arakawa and Schubert 1974). Correspondingly, a typical vertical profile of $(Q_1 - Q_2 - Q_R)$ in convective situations has positive values aloft and negative values near the surface (Yanai et al. 1976).

Convection consumes CAPE and therefore drives the atmosphere from a statically unstable state toward a statically neutral or stable state. In the framework of GCAPE (Randall and Wang 1992; Wang and Randall 1994), this means that convection drives the atmosphere from the given state toward the "reference state."

Let $h_g(p)$ and $h_r(p)$ be the moist static energy profiles of the atmosphere in the given state and the GCAPE reference state, respectively. We assume that

$$(Q_1 - Q_2 - Q_R) = \frac{(h_r - h_g)}{\tau_{\text{adj}}}. \tag{2}$$

Here τ_{adj} is an adjustment timescale, which is nonnegative and not necessarily constant. In (2), we follow Betts (1986) by assuming that the atmosphere is adjusting toward the reference quasi-equilibrium state over a finite time. After some experimentation, Betts and Miller (1986) assumed a fixed value of 2 hours for the adjustment time in their scheme. As explained below, we allow τ_{adj} to vary with time.

We use a modified version of Lorenz's parcel-moving algorithm to find the reference state and, therefore, h_r. See Randall and Wang (1992) and Wang and Randall (1994) for a detailed description of the algorithm. In the next section we explain how we determine τ_{adj}. Having obtained τ_{adj}, we can compare $(h_r - h_g)/\tau_{\text{adj}}$ with the observed $(Q_1 - Q_2 - Q_R)$. Figure 1 shows the vertical profiles of both quantities averaged over the "disturbed" portions of GATE Phase III. The agreement is encouraging. Further discussion of these results is given in section 6.

3. Finding τ_{adj}

We determine the vertically uniform τ_{adj} needed to make $(h_r - h_g)/\tau_{\text{adj}}$ as close as possible to the observed $(Q_1 - Q_2 - Q_R)$ for each of the GATE Phase III observation times. We choose the τ_{adj} that minimizes the vertical integral of the root-mean-square difference between $(h_r - h_g)/\tau_{\text{adj}}$ and $(Q_1 - Q_2 - Q_R)$. For some undisturbed soundings, the "best" τ_{adj} as determined

[1] The cloud model used by Nitta is an entraining plume model of the type used in the AS parameterization. Emanuel (1991) has criticized the use of entraining plume models in cumulus parameterizations. Recent work by Lin (1994) suggests, however, that these models can in fact serve as realistic agents of convective transports.

in this way is very large. Those soundings whose "best" τ_{adj} is found to be larger than 50 hours are assigned $\tau_{adj} = 50$ h for plotting purposes.

Figure 2 shows the "best" τ_{adj}'s plotted against the rate of GCAPE production by large-scale processes, including horizontal and vertical advection and radiative heating, for all of GATE Phase III observations. Here the rate of GCAPE production by large-scale processes has been determined as follows. First we determine the GCAPE associated with an observed sounding. Then we assume that the large-scale processes act on the observed sounding over a time interval Δt. In this way, a hypothetical sounding is obtained. The difference of the GCAPE between the hypothetical sounding and the observed sounding, divided by Δt, is the rate of GCAPE production by large-scale processes. We choose $\Delta t = 3$ h simply because the observations are available every three hours. Wang and Randall (1994) showed that there is a high positive correlation between the GCAPE production rate by large-scale processes and the observed precipitation rate during GATE Phase III.

Surface evaporation makes an important contribution to the GCAPE production rate, but nevertheless it is not well correlated with cloud activity (Wang and Randall 1994). For this reason, we do not expect surface evaporation to be well correlated with τ_{adj}, and so, when we relate τ_{adj} to the large-scale forcing, we do not consider surface evaporation. In an average or "background" sense the evaporation is a major CAPE generator, but temporal fluctuations of the evaporation rate do not play a major role in the fluctuations of the total CAPE generation rate, at least in the GATE dataset. This point needs further study.

Figure 2 shows that for most of the disturbed cases (with large precipitation rates or rapid GCAPE production rates), τ_{adj} is several hours larger than the 2-h adjustment time used in the Betts–Miller parameterization.

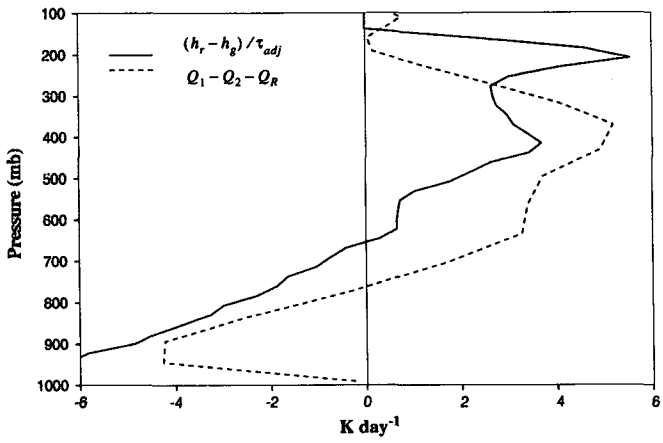

FIG. 1. The averaged vertical distributions of $(h_r - h_R)/\tau_{adj}$ and the observed $(Q_1 - Q_2 - Q_R)$ for the 64 "disturbed" GATE Phase III observations that have precipitation rates larger than 12 mm day^{-1}. Here τ_{adj} is determined from (3).

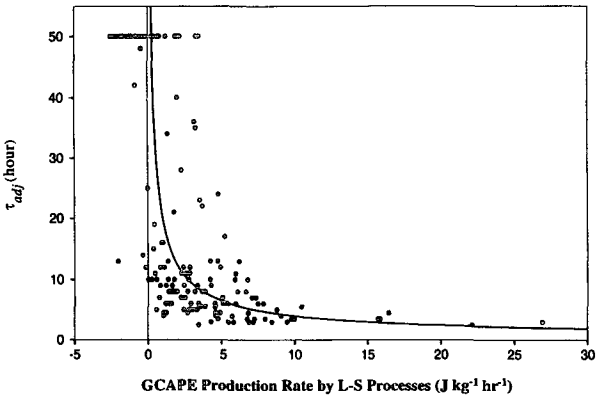

FIG. 2. A comparison of the "best" τ_{adj} against the GCAPE production rate by large-scale processes, including advection, vertical adiabatic expansion, and radiative cooling. Each point represents each observation time of GATE Phase III. The solid curve represents an empirical relation between the "best" τ_{adj} and the GCAPE production rate.

It also can be seen from Fig. 2 that, for most of the observations, larger GCAPE production rates correspond to smaller values of τ_{adj}, while smaller GCAPE production rates correspond to larger values of τ_{adj}. This means that for disturbed periods (with larger GCAPE production rates), there is strong large-scale forcing and vigorous convection. The feedback due to convection is strong, so that the atmosphere rapidly relaxes toward the reference state. Therefore, τ_{adj} is smaller for these times. In contrast, for the undisturbed periods, the large-scale forcing, and therefore convection and its feedback, are weak; the atmosphere relaxes more slowly toward the reference state, and so τ_{adj} is larger.

Based on Fig. 2, we propose here an empirical relationship between τ_{adj} and the GCAPE production rate by large-scale processes, as shown by the solid curve in Fig. 2:

$$\tau_{adj} = 20\,(\mathrm{dGCAPE})^{-0.7}. \qquad (3)$$

Here dGCAPE is the GCAPE production rate by large-scale processes (in units of J kg^{-1} h^{-1}), and τ_{adj} is adjustment time (in units of hours). We acknowledge that, from the point of view of dimensional analysis, this relationship cannot be universal.

In semiprognostic tests with GATE Phase III data, presented later, the GCAPE production rate by large-scale processes can be calculated for each observational time. Then a value of τ_{adj} can be obtained from (3). This method is not useful in a prognostic model, however, because the GCAPE production rate by large-scale processes cannot easily be determined due to

some conceptual[2] as well as practical problems. For possible model use, we relate τ_{adj} to the cumulus kinetic energy (CKE). The CKE can be predicted in a model (Randall and Pan 1993). Figure 3 shows a comparison between τ_{adj} and the CKE based on simulations performed with the UCLA Cumulus Ensemble Model (CEM). Two CEM cases are selected here: a GATE simulation and a weak wind shear simulation (case Q03 of Xu et al. 1992). Figure 3 shows that larger CKE corresponds to smaller τ_{adj}, while smaller CKE corresponds to larger τ_{adj}. An empirical relationship between τ_{adj} and CKE,

$$\tau_{adj} = 300(\mathrm{CKE})^{-1.2}, \qquad (4)$$

is shown in Fig. 3. Here again the CKE is in joules per squared meter and τ_{adj} is in hours.

After obtaining τ_{adj}, we can compute $(h_r - h_g)/\tau_{adj}$ and compare it to the observed $(Q_1 - Q_2 - Q_R)$. First, for the undisturbed periods of GATE, the observed $(Q_1 - Q_2 - Q_R)$ (not shown) is mostly positive throughout the troposphere and is larger in the lower half of the troposphere. This indicates that there was no organized deep convection at these times. Observational studies (Nitta 1978; Thompson et al. 1979; Nicholls and LeMone 1980) show that at these undisturbed times shallow clouds and planetary boundary-layer turbulence occurred, but organized deep convection was rarely found.

On the other hand, even for the undisturbed periods, the GCAPE algorithm still finds that the boundary-layer air in the given state can and must penetrate to the upper troposphere in order to produce the reference state, just as for the disturbed periods. Since we use a large τ_{adj} for these undisturbed times, the effects of the deep clouds are predicted to be weak, and so the model results are in agreement with the observations.

4. Data

We use the GATE Phase III data, as analyzed by Yanai's group at the University of California at Los Angeles. Sui et al. (1989) and Wu (1993) give detailed descriptions of the data. Here, we use only the mean sounding over the 1° × 1° box at the center of GATE ship array. The data correspond to 160 observation times, spanning every three hours from 0000 UTC 30 August to 2100 UTC 18 September 1974.

Simulated domain-average results from the UCLA Cumulus Ensemble Model (CEM), as developed by Krueger (1988), are also used here. The simulated results span every hour for 11 days. The horizontal domain size is 512 km, and the depth of the domain is 19 km. A weak wind shear case is selected (Q03 case of Xu et al. 1992). See Xu et al. (1992) for a detailed description of the model and its results.

In this paper, "disturbed" periods are taken to be those with precipitation rates larger than 12 mm day^{-1}.

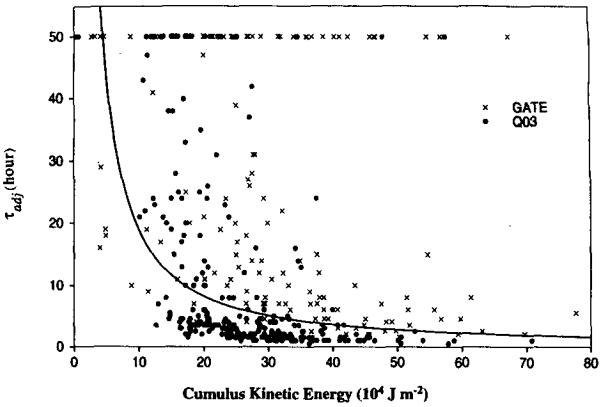

FIG. 3. A comparison of the "best" τ_{adj} against cumulus kinetic energy (CKE) for simulations from the UCLA Cumulus Ensemble Model (CEM). Two CEM cases are used: GATE and a weak wind shear simulation (case Q03 of Xu et al. 1992). An empirical relationship between the "best" τ_{adj} and CKE is shown as the solid curve.

5. Preliminary tests

Now refer back to Fig. 1, which shows the averaged vertical distributions of $(h_r - h_g)/\tau_{adj}$ and the observed $(Q_1 - Q_2 - Q_R)$ for the 64 disturbed observations during GATE Phase III. In Fig. 1, τ_{adj} is determined from (3). The figure shows that both $(h_r - h_g)/\tau_{adj}$ and the observed $(Q_1 - Q_2 - Q_R)$ exhibit the signature of convection: positive values in the upper and midtroposphere and negative values in the lower troposphere. Two obvious differences are also seen between $(h_r - h_g)/\tau_{adj}$ and the observed $(Q_1 - Q_2 - Q_R)$: one difference is in the upper troposphere, where $(h_r - h_g)/\tau_{adj}$ has a large peak, while $(Q_1 - Q_2 - Q_R)$ does not. The other is in the boundary layer, where the negative value of $(h_r - h_g)/\tau_{adj}$ is too large compared with the observed $(Q_1 - Q_2 - Q_R)$.

The inconsistency between $(h_r - h_g)/\tau_{adj}$ and $(Q_1 - Q_2 - Q_R)$ in the boundary layer is due to the fact that the effects of surface energy flux into the planetary boundary layer (PBL) have not been included in the computation of $(h_r - h_g)/\tau_{adj}$. In addition, the vertical integral of $(h_r - h_g)/\tau_{adj}$ has to be zero because of the definition of the reference state and the conservation of moist static energy, while the vertical integral of the observed $(Q_1 - Q_2 - Q_R)$ is strongly positive. If we included a PBL parameterization, as we surely would in any numerical model, then the value of $(h_r - h_g)/\tau_{adj}$ in the boundary layer would increase, becoming closer to the observed $(Q_1 - Q_2 - Q_R)$.

[2] For instance, it is not clear whether we should treat the effects of the stratiform clouds associated with cumulus convection and the radiative cooling associated with cumulus anvil clouds as part of the large-scale forcing or as part of the convective feedback (Randall and Pan 1993; Pan 1995).

6. Detrainment

The peak of $(h_r - h_g)/\tau_{adj}$ in the upper troposphere is mainly caused by the strong compensating "return flow" in the layers just below the "cloudy layers." By "cloudy layers" we mean layers that contain condensed water in the reference state because they are occupied by parcels coming from lower layers in the given state; "return flow" means the subsidence needed to reach the reference state in those layers that are occupied by parcels coming from higher levels in the given state. The upper-tropospheric peak of $(h_r - h_g)/\tau_{adj}$ does not appear in the observed $(Q_1 - Q_2 - Q_R)$.

When we try to understand this discrepancy, we should keep in mind that although convection drives the atmosphere from the given state toward the reference state, it will not fully succeed even in the absence of large-scale forcing. As soon as the boundary-layer air moves up toward its position in the reference state, entrainment of air from the intervening environmental layers and the pressure force associated with the vertical convergence of cloudy air near cloud top make some of the penetrating air detrain before reaching its reference-state level. Air that has been detrained from a convective cell may form an anvil cloud in the upper and midtroposphere. During GATE, extensive anvil clouds were observed in the mid- and upper troposphere (Houze and Betts 1981). These observations suggest that during GATE a large amount of cloudy air was detrained from convective cells before reaching its adiabatic neutral buoyancy level in the upper troposphere. In our GCAPE algorithm, however, we assume that *all* of the penetrating air reaches its reference-state position in the upper troposphere and stays there.

Therefore, to obtain better agreement between $(h_r - h_g)/\tau_{adj}$ and the observed $(Q_1 - Q_2 - Q_R)$, we must modify the adjusted state to take into account the effects of some irreversible processes, including entrainment and detrainment, PBL turbulence and shallow convection, and precipitation and re-evaporation of condensed water. Here we suggest a very simple and ad hoc approach to include detrainment effects and show that the results are somewhat improved.

Figures 4a and 4b show how cloudy air is assumed to be redistributed from the given state to the reference state. Figure 4a shows the given state in which some air in the lower troposphere (the darker section) needs to penetrate to the upper troposphere to reach its reference state position. Figure 4b shows the reference state in which the lower tropospheric air of the given state has reached its reference state position in the upper troposphere to form cloud there, as shown by the shading; in compensation, all other air has subsided level by level. In this case, all cloudy air is at its adiabatic neutral buoyancy level in the idealized reference state. We call the cloud in Fig. 4b a "horizontally uniform" anvil. The corresponding vertical distribution of

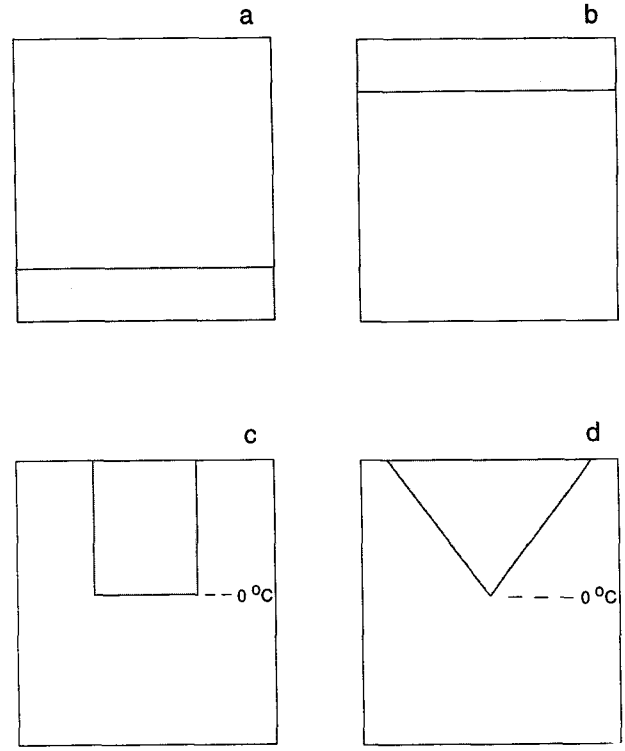

FIG. 4. The schematic diagrams for (a) the given state in which the air mass of the lower portion (the shading section) needs to be moved up to the top portion in the reference state; (b) the theoretical reference state in which the cloudy air forms a horizontally uniform anvil cloud in the top portion of the diagram; (c) the "modified" reference state in which the cloudy air forms a "rectangular" anvil cloud with its top at the adiabatically neutral buoyancy level and its bottom at the melting (0°C) level; (d) the "modified" reference state in which the cloudy air forms a "triangular" anvil cloud with its top at the adiabatically neutral buoyancy level and its bottom at the melting (0°C) level.

$(h_r - h_g)/\tau_{adj}$ has already been shown in Fig. 1. We now suggest a very simple approach to replace the idealized cloud of Fig. 4b with something more like a real cloud, so that the idealized reference state as shown in Fig. 4b is correspondingly modified to a more realistic adjusted state.

As mentioned above, some of the penetrating air detrains from the convective cells before reaching its adiabatic neutral buoyancy level, which for GATE is in the upper troposphere. We try to relate the vertical distribution of detrainment to the "shape" of the anvil cloud. For simplicity, we assume that the air at a given height in the anvil cloud comes only from the subensemble that detrains at the same height. This assumption makes it possible for us to determine how an upward-penetrating parcel distributes its mass between the bottom and top levels of the anvil cloud in order to form a particular anvil shape. For instance, if the mass of an upward-penetrating parcel is detrained at the same rate from the bottom level to the top level of the anvil, a rectangular anvil will be produced.

It is reasonable to assume that the air at a given height in the anvil cloud comes only from the cloud elements that detrain at the same height because although there are mesoscale vertical motions in anvil clouds, they are much weaker than those active in convective updrafts. Cheng and Yanai (1989) showed that the effects of eddy fluxes associated with anvil clouds are very small compared to the condensation and evaporation effects.

Our approach here is to assume the shape of the anvil cloud in order to determine detrainment profile. Observational studies of anvil clouds (e.g., Zipser 1977; Leary and Houze 1979; Houze et al. 1981; Johnson and Young 1983) show that tropical and warm-season anvils extend from the melting (0°C) level to the adiabatic neutral buoyancy level. This motivates us to assume that the top and bottom of the anvil cloud are at the adiabatic neutral buoyancy level and melting (0°C) level, respectively. This assumption restricts the applicability of our parameterization to tropical and warm-season midlatitude convection.

The lateral shape of the anvil cloud is not as well known as its top and bottom levels, however. Here, we consider two extreme situations. As one possibility, we consider an anvil cloud with a "rectangular" form in the reference state. Figure 4c shows such a modified adjusted state. To find this modified adjusted state, we assume that the convectively lifted air is uniformly detrained between the melting level and the adiabatic neutral-buoyancy level. If there are N layers between the melting level and the adiabatic neutral buoyancy level, a fraction $1/N$ of the convectively lifted air is detrained into each of these layers to form anvil cloud there. In association with this detrainment, a downward layer by layer return flow is correspondingly reduced by $1/N$ in each layer upward from the melting level to the adiabatic neutral-buoyancy level because the upward-penetrating flow is reduced by a factor of $1/N$ across each layer. In this modified adjusted state, each layer between the top and bottom of the anvil cloud includes some of the detrained cloudy mass (which forms an anvil cloud there), together with some air contributed by the compensating return flow from layers above, and also possibly some mass remaining in the layer from the given state. The air in each anvil layer in the adjusted state is made up of some combination of these three components.

As a second possibility, we consider an anvil cloud with a "triangular" form. Figure 4d shows the correspondingly modified adjusted state. To find this modified adjusted state, we define a parameter, α, such that a fraction α of the mass of each penetrating parcel is detrained in the bottom layer of the anvil (0°C level). In the layers above, the detrainment rate increases upward at a fractional rate of 2α, all the way to the top of the anvil. Correspondingly, the downward layer by layer return flow is reduced by the fraction 2α upward from the bottom to the top of the anvil.

The τ_{adj} computed from (3) is based on the horizontally uniform anvil cloud. If we modify the adjusted state to correspond to the "rectangular" or "triangular" anvil clouds, we should recompute τ_{adj} accordingly. We did this by following Fig. 2. It turns out that the empirical relationships between τ_{adj} and the GCAPE production rate by large-scale processes for the "rectangular" and "triangular" anvil cloud cases are very close to that of the horizontally uniform anvil cloud case. Thus, we continue to use (3) for the "rectangular" and "triangular" anvil clouds.

Figure 5 shows the vertical distributions of $(h_r - h_g)/\tau_{adj}$ for the modified adjusted states obtained with the rectangular and triangular anvils. For comparison, the vertical distributions of $(h_r - h_g)/\tau_{adj}$ for the "horizontally uniform" anvil cloud, as shown in Fig. 1, is also plotted in Fig. 5. With the "horizontally uniform" anvil, $(h_r - h_g)/\tau_{adj}$ is much larger than the observed $(Q_1 - Q_2 - Q_R)$ above 275 mb and is smaller than the observed $(Q_1 - Q_2 - Q_R)$ between 275 and 600 mb. With the rectangular and triangular anvils, $(h_r - h_g)/\tau_{adj}$ is reduced above 275 mb and increased between 275 and 600 mb so that the agreement with the observed $(Q_1 - Q_2 - Q_R)$ in the upper and middle troposphere improves.

7. Results from a semiprognostic test with GATE Phase III data

A cumulus parameterization can be subjected to a semiprognostic test, which can be performed by using either observational data or simulation results (e.g., Lord 1982; Xu and Arakawa 1992). A semiprognostic test is a one-step prediction of the cumulus heating and drying rates based on given large-scale conditions. For each observation time, the observed estimates of ad-

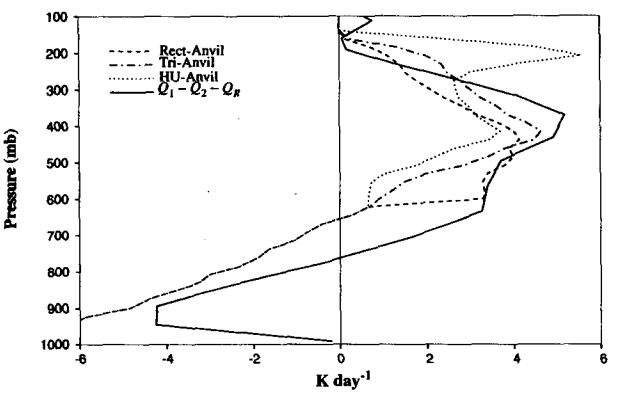

FIG. 5. Same as Fig. 1 except that the moist static energy of the reference state, h_r, is for the "modified" adjusted state with the "rectangular" anvil cloud (Rect-Anvil) as shown in Fig. 4c and with the "triangular" anvil cloud (Tri-Anvil) as shown in Figure 4d. As a comparison, the averaged vertical distributions of $(h_r - h_g)/\tau_{adj}$ for the horizontally uniform anvil cloud (HU-Anvil) as shown in Fig. 4b is also shown.

vective tendencies and radiative heating are used to estimate the large-scale forcing. The observations and the cumulus parameterization are combined to determine the cumulus mass-flux spectrum. The associated precipitation rate and cumulus warming and drying are then calculated from the predicted mass flux spectrum. They do not influence the large-scale variables as they would in a fully prognostic test, however, because the semiprognostic test does not march in time (as a fully prognostic test does). In this way, a semiprognostic test isolates errors caused by the cumulus parameterization from those caused by other components of the large-scale numerical model. As noted, for example, by Betts and Miller (1986), heating and drying profiles derived from semiprognostic or diagnostic tests can be quite different from the profiles obtained as the convective parameterization and a host model march in step. Both prognostic and semiprognostic tests are needed to fully evaluate a parameterization.

We have performed a semiprognostic test with GATE Phase III. In the discrete model, we divide each sounding into 40 layers, and the cloudbase level is assumed to be at 950 mb. We did three kinds of computations: 1) with the "horizontally uniform" anvil cloud (as shown in Fig. 4b); 2) with the "rectangular" anvil cloud (as shown in Fig. 4c); and 3) with the "triangular" anvil cloud (as shown in Fig. 4d). Figure 6 shows the time variations of the calculated precipitation rates for GATE Phase III. The time variation of the radar-observed precipitation rate for GATE Phase III is also shown for comparison. Figures 7a and 7b show the time-averaged vertical distributions of cumulus warming ($Q_1 - Q_R$) and drying (Q_2), respectively, for GATE Phase III.

Figures 6 and 7 show that our results are in reasonable agreement with the observations. Although the three different anvil cloud parameterizations do not give large differences in the calculated precipitation rates, they do influence the vertical distributions of cumulus warming and drying. The cumulus warming and drying in the upper troposphere for the "horizontally uniform" anvil cloud are stronger than those for the "rectangular" and "triangular" anvil clouds. The excessive calculated cumulus warming and drying in the midtroposphere may be caused by our neglect of melting and the evaporation of precipitation. Because we have not included the effects of shallow convective clouds, even though such shallow convection is important in GATE, especially in the undisturbed periods (e.g., Nitta 1978; Thompson et al. 1979), the calculated cumulus warming and drying in the lower half of troposphere are weaker than observed.

8. Concluding discussion

A cumulus parameterization for large-scale models has been presented. It is an adjustment scheme. The reference state associated with the GCAPE is the end-state of the convective adjustment. This reference state varies from case to case depending on the given soundings. The timescale for the adjustment also varies, ranging from several hours to several tens of hours, depending on the intensity of the large-scale forcing. Because the adjustment timescale is related to the

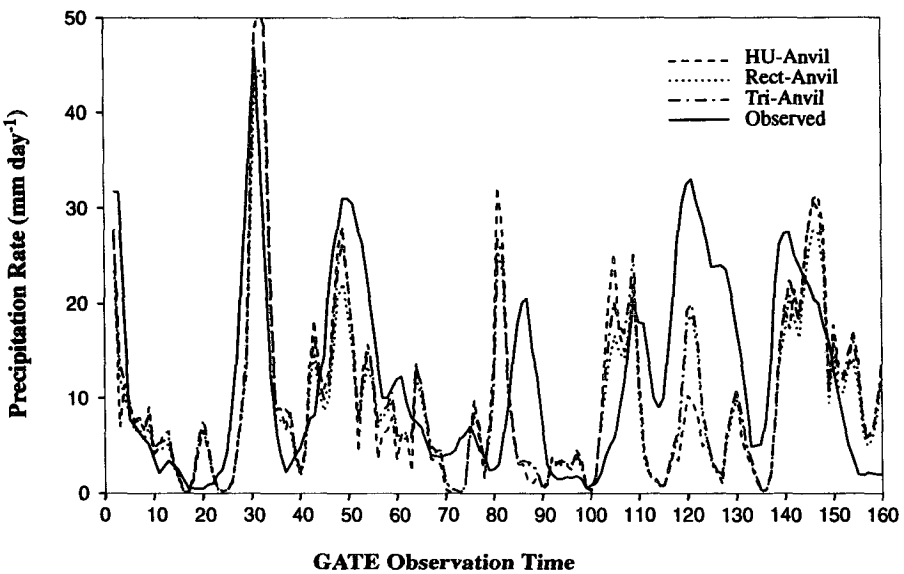

FIG. 6. The time variations of calculated and radar-observed precipitation rates for GATE Phase III observations. Three calculated precipitation rates are presented: 1) with the horizontally uniform anvil cloud (HU-Anvil) as shown in Fig. 4b; 2) with the "rectangular" anvil cloud (Rect-Anvil) as shown in Fig. 4c; and 3) with the "triangular" anvil cloud (Tri-Anvil) as shown in Fig. 4d.

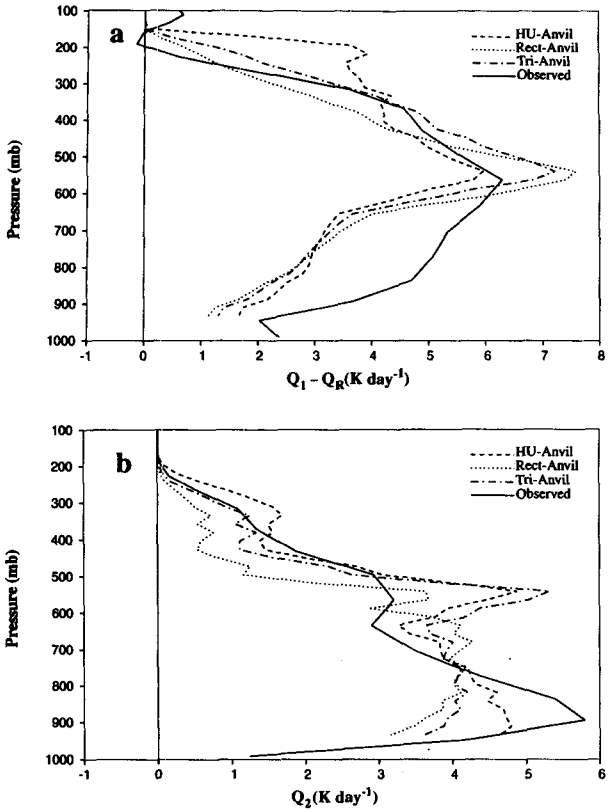

FIG. 7. (a) The averaged vertical distributions of calculated and "observed" cumulus warming ($Q_1 - Q_R$) for the GATE Phase III observations. Three calculated cumulus warming are presented: 1) with the horizontally uniform anvil cloud (HU-Anvil) as shown in Fig. 4b; 2) with the "rectangular" anvil cloud (Rect-Anvil) as shown in Fig. 4c; and 3) with the "triangular" anvil cloud (Tri-Anvil) as shown in Fig. 4d. (b) The same as (a) except for cumulus drying (Q_2).

large-scale forcing, the intensity of convective activity is determined by the large-scale forcing as in the Arakawa–Schubert parameterization. The methods of Nitta (1975) and Johnson (1976) are combined to diagnose the convective heating and drying rates.

The closure assumption of the present parameterization is (2), which can be written as

$$\left(\frac{\partial h}{\partial t}\right)_{CU} = \frac{h_r - h}{\tau_{adj}}. \tag{5}$$

Although (5) looks similar to the closure assumptions of Betts (1986), which are

$$\left(\frac{\partial T}{\partial t}\right)_{CU} = \frac{T_{ref} - T}{\tau_{adj}} \tag{6}$$

and

$$\left(\frac{\partial q}{\partial t}\right)_{CU} = \frac{q_{ref} - q}{\tau_{adj}}, \tag{7}$$

where T is temperature q is total water mixing ratio and the subscript "ref" denotes the quasi-equilibrium reference state profiles, some important differences exist. An important difference is that we allow τ_{adj} to change from case to case depending on the large-scale forcing, while Betts and Miller (1986) use a prescribed constant τ_{adj}. In our parameterization, when the large-scale forcing is strong, τ_{adj} is small; and so the effects of convection are strong. On the other hand, when the large-scale forcing is weak or negative, a large τ_{adj} is used, and so convection is inhibited. In this way, the intensities of cloud activity and precipitation are related to the large-scale forcing.

The criterion for activating the Betts–Miller parameterization is that positive buoyancy is encountered when a hypothetical cloud parcel is lifted adiabatically from the boundary layer. However, as it has been shown (Thompson et al. 1979; Wang and Randall 1994) that in GATE the observed precipitation rate is positively correlated with the intensity of large-scale forcing but negatively correlated with the CAPE. This means that it may be more realistic to relate the effects of convection to the large-scale forcing than to the amount of CAPE.

Although both the Betts–Miller parameterization and the present parameterization are relaxation schemes, the final reference states are different. Betts (1986) determined the equilibrium state empirically from observed soundings. The equilibrium state of our parameterization is determined by the given soundings and the GCAPE theory, modified to include the effects of detrainment below the neutral buoyancy level.

A key difference between our parameterization and the Arakawa–Schubert (AS) parameterization is in the calculation of the cloudbase mass flux. In the AS parameterization, the quasi-equilibrium assumption is used to calculated the cloudbase mass flux. The quasi-equilibrium assumption requires that, at any moment, the rate of production of CAPE by large-scale forcing is balanced by the consumption of CAPE by convection, so that after each time step the CAPE remains unchanged. A cloud model is used to measure conditional instability and to define the reference state.

In our parameterization, no cloud model is needed to find the reference state. The effects of convection on the moist static energy are obtained from (2). Then, by using Nitta's method, we determine the effects of convection on the temperature and moisture fields. Both the AS parameterization and our parameterization relate the intensity of convection to the large-scale forcing but in different ways. The present parameterization is a relaxation scheme in which no exact balance is required.

We do not adjust directly to the temperature, moisture, and condensed water of the reference state because this state is highly unrealistic, especially in view of high condensed water contents in the upper troposphere. We have considered the following strategy,

however: on a given time step, adjust the temperature, moisture, and condensed water some fraction of the way to the reference state. Then, within the same time step, allow a microphysics parameterization to reduce the condensed water concentration in the upper troposphere by precipitation and to increase the water vapor content of the lower troposphere by evaporating the falling rain. This approach would still include a "cloud model" in the sense that we would have parameterizations of precipitation, evaporation, and so on. Future explorations may go in this direction.

We regard this as an exploratory study. Certainly much additional work is needed before the ideas here are ready for application in large-scale models. Nevertheless, we are encouraged by our results to date and feel that this approach merits further investigation.

Acknowledgments. We thank Dr. Xiaoqing Wu of the National Center for Atmospheric Research (NCAR) for providing the GATE Phase III data as analyzed by Prof. Yanai's group at UCLA, Dr. Kuan-Man Xu of CSU for providing the simulated data from the CEM, and Dr. Ernest E. Recker of the University of Washington for providing the GATE Phase III radar-observed precipitation data.

Support has been provided by the National Aeronautics and Space Administration under Grant NAG5-1058 and the National Science Foundation under Grant ATM-8907414, both to Colorado State University. Computing resources were provided by the Scientific Computing Division of NCAR, which is sponsored by the National Science Foundation.

APPENDIX

Nitta's Diagnostic Model for the Cumulus Feedbacks

Nitta (1975) designed a scheme to calculate the cloudbase mass flux. Following Ooyama (1971), Yanai et al. (1973), and Arakawa and Schubert (1974), the large-scale heat and moisture budgets satisfy

$$\rho(Q_1 - Q_R) = D(\hat{s}_c - \bar{s}) - LD\hat{l} + M_c \frac{\partial \bar{s}}{\partial z}, \quad \text{(A1)}$$

$$-\rho Q_2 = LD(\hat{q}_c - \bar{q} + \hat{l}) + LM_c \frac{\partial \bar{q}}{\partial z}. \quad \text{(A2)}$$

Here $s \equiv c_pT + gz$, the sum of the enthalpy and potential energy, is the dry static energy; q is the water vapor mixing ratio; $\hat{s}_c$, $\hat{q}_c$, and $\hat{l}$ are dry static energy, mixing ratio of water vapor, and mixing ratio of liquid water of clouds at the detrainment level; ρ is density of the air; Q_1 is the apparent heating source; Q_2 is the apparent moisture sink (Yanai et al. 1973); Q_R is the radiative heating rate; and L is the latent heat of condensation. Horizontal large-scale averages are denoted by overbars. By using the spectral cloud model of Arakawa and Schubert (1974), the total cloud mass flux $M_c(z)$ and total detrainment $D(z)$ can be represented in the following spectral forms:

$$M_c(z) = \int_0^{\lambda_{D(z)}} m(z, \lambda)d\lambda = \int_0^{\lambda_{D(z)}} m_B(\lambda)\eta(z, \lambda)d\lambda, \quad \text{(A3)}$$

$$D(z) = m_B[\lambda_D(z)]\eta[z, \lambda_D(z)]\left[-\frac{d\lambda_D(z)}{dz}\right]. \quad \text{(A4)}$$

Here λ is the fractional rate of entrainment, which is assumed to be constant with height for each cloud type. The function $m_B(\lambda)$ is called the cloudbase mass-flux distribution function. Here $\eta(z, \lambda)$ is the normalized vertical profile of the λth subensemble mass flux at height z.

If we add (A1) to (A2) and use (A3) and (A4), we obtain an integral equation for $m_B(\lambda)$, the cloudbase mass-flux distribution function, as

$$\int_0^{\lambda_{D(z)}} m_B(\lambda)\eta(z, \lambda)d\lambda - (\hat{h}_c - \bar{h})\left(\frac{\partial \bar{h}}{\partial z}\right)^{-1} \times \eta[z, \lambda_D(z)]\left[\frac{d\lambda_D(z)}{dz}\right]m_B[\lambda_D(z)] = \rho\left(\frac{\partial \bar{h}}{\partial z}\right)^{-1}(Q_1 - Q_2 - Q_R). \quad \text{(A5)}$$

Here $h = s + Lq$ is the moist static energy, and $\hat{h}_c$ is the moist static energy of clouds at the detrainment level. By solving (A5), $m_B(\lambda)$ can be obtained as long as the other large-scale quantities in (A5), including $(Q_1 - Q_2 - Q_R)$, are known. This is what Nitta (1975) did.

In Nitta's (1975) scheme, the effects of downdrafts were not included. Although Nitta considered downdraft effects in his later schemes (Nitta 1977, 1978), closure could only be achieved if Q_1 and Q_2 were known separately. In our scheme we can diagnose $(Q_1 - Q_2 - Q_R)$ from (2), but not Q_1 and Q_2 individually. Therefore, we use Johnson's (1976) simple approach to include the effects of downdrafts.

Johnson (1976) assumed that each updraft has an accompanying downdraft and that both have the same fractional mass entrainment rate, λ. He also assumed that the downdrafts originate at a level above cloudbase and below cloud top, given by a certain fraction β of the pressure depth of the corresponding updraft. A relation between the downdraft–origination-level mass-flux $M_0(\lambda)$ and the updraft–cloudbase mass-flux $M_B(\lambda)$, $M_0(\lambda)/M_B(\lambda) = -\epsilon(\lambda)$, was used. Here $M_B(\lambda) = m_B(\lambda)d\lambda$ is the cloud mass flux of the λth subensemble at the cloudbase. We follow Johnson (1976) by choosing $\beta = 0.75$ and $\epsilon(\lambda) = 0.3$.

Using Johnson's (1976) assumptions, (A5) becomes

$$\int_0^{\lambda_D(z)} m_B(\lambda)[\eta_u(z,\lambda) - \epsilon(\lambda)\eta_d(z,\lambda)]d\lambda - (\hat{h}_u - \bar{h})\left(\frac{\partial \bar{h}}{\partial z}\right)^{-1}\eta_u[z,\lambda_D(z)] \times \left[\frac{d\lambda_D(z)}{dz}\right]m_B[\lambda_D(z)] = \rho\left(\frac{\partial \bar{h}}{\partial z}\right)^{-1}(Q_1 - Q_2 - Q_R). \quad \text{(A6)}$$

Here the subscript u denotes the updraft and the subscript d denotes the downdraft, and a circumflex ($\hat{}$) denotes a detrainment quantity. After we obtain $m_B(\lambda)$ from (A6), we can calculate the precipitation rate and the large-scale temperature and moisture changes at each level due to cumulus convection ($Q_1 - Q_R$ and Q_2, respectively). Here we follow the scheme of Lord et al. (1982) but extend it to include downdrafts. Any negative mass fluxes are replaced by zero. In such cases (A6) is only approximately satisfied.

Briefly, when the effects of downdrafts are included, the environmental air is entrained not only to the updrafts but also to the downdrafts. Also, there exist both the environmental subsidence for compensating updrafts and the environmental ascent to compensate downdrafts. The cumulus precipitation of updrafts is calculated by using the method of Lord et al. (1982), but some of the precipitation is reevaporated within the downdrafts. The downdrafts are assumed to be saturated without condensate at the cloudbase level. By using the conservation of moist static energy, the temperature of downdraft at the cloudbase level can be obtained. Then the water vapor mixing ratio (saturated) of the downdraft at the cloud-base level can be obtained. This water vapor mixing ratio increase in the downdraft from the level of origin to cloudbase is made possible by the re-evaporation of some of the precipitation produced by the updrafts and also by the moisture supply from the environment through lateral entrainment. After the moisture supply from environment through lateral entrainment has been calculated, the reevaporation of precipitation within downdrafts can be obtained. The final cumulus precipitation rate equals the precipitation rate produced by updrafts minus the rate of re-evaporation of precipitation within downdrafts. Wang (1994) gives a detailed description of this model.

Nitta's scheme has some deficiencies. Practically, to make (A6) solvable for the cloudbase mass flux, we must start the calculation from the highest model level. The value of $(Q_1 - Q_2 - Q_R)$ at the highest level determines the intensity of cloud-base mass flux of the clouds that detrain at the highest level. If for some reason the value of $(Q_1 - Q_2 - Q_R)$ is too large at this level, the cloudbase mass flux for the highest clouds will be too strong. As a result, the cloudbase mass flux for the clouds that detrain at lower levels will be underestimated. Similarly, if the value of $(Q_1 - Q_2 - Q_R)$ at a higher level is too small, the intensity of the cloudbase mass flux of shallower clouds will be too strong. This means that, in Nitta's model, the values of $(Q_1 - Q_2 - Q_R)$ aloft have more influence than those near the surface. In addition, the results depend on the plume model (Arakawa and Schubert 1974). The cloudbase mass flux obtained can be accepted only when λ decreases with height (Nitta 1975).

REFERENCES

Arakawa, A., and W. H. Schubert, 1974: The interaction of a cumulus cloud ensemble with large-scale environment. Part I. *J. Atmos. Sci.*, **31,** 674–701.

Betts, A. K., 1986: A new convective adjustment scheme. Part I: Observational and theoretical basis. *Quart. J. Roy. Meteor. Soc.*, **112,** 677–691.

——, and M. J. Miller, 1986: A new convective adjustment scheme. Part II: Single column tests using GATE wave, BOMEX, ATEX, and arctic air-mass data sets. *Quart. J. Roy. Meteor. Soc.*, **112,** 693–709.

Cheng, M.-D., 1989: Effects of downdrafts and mesoscale convective organization on the heat and moisture budgets of tropical cloud clusters. Part II: Effects of convective-scale downdrafts. *J. Atmos. Sci.*, **46,** 1540–1564.

——, and M. Yanai, 1989: Effects of downdrafts and mesoscale convective organization on the heat and moisture budgets of tropical cloud clusters. Part III: Effects of mesoscale convective organization. *J. Atmos. Sci.*, **46,** 1566–1588.

Emanuel, K. A., 1991: A scheme for representing cumulus convection in large-scale models. *J. Atmos. Sci.*, **48,** 2313–2335.

Houze, R. A., Jr., and A. K. Betts, 1981: Convection in GATE. *Rev. Geophys. Space Phys.*, **19,** 541–576.

——, S. G. Geotis, F. D. Marks, and A. E. West, 1981: Winter monsoon convection in the vicinity of North Borneo. Part I: Structure and time variation of the clouds and precipitation. *Mon. Wea. Rev.*, **108,** 1595–1614.

Johnson, R. H., 1976: The role of convective-scale precipitation downdrafts in cumulus and synoptic-scale interactions. *J. Atmos. Sci.*, **33,** 1890–1910.

——, and G. S. Young, 1983: Heat and moisture budgets of tropical mesoscale anvil clouds. *J. Atmos. Sci.*, **40,** 2138–2147.

Krishnamurti, T. N., and W. J. Moxim, 1971: On parameterization of convective and nonconvective latent heat release. *J. Appl. Meteor.*, **10,** 3–13.

Krueger, S. K., 1988: Numerical simulation of tropical cumulus clouds and their interaction with the subcloud layer. *J. Atmos. Sci.*, **45,** 2221–2250.

Kurihara, Y., 1973: A scheme of moist convective adjustment. *Mon. Wea. Rev.*, **101,** 547–553.

Leary, C. A., and R. A. Houze, Jr., 1979: Melting and evaporation of hydrometeors in precipitation from the anvil clouds of deep tropical convection. *J. Atmos. Sci.*, **36,** 669–679.

Lin, C., 1994: Development of an improved cloud model for use in cumulus parameterization. Ph.D. thesis, University of California, Los Angeles, 252 pp.

Liu, Y.-Z., 1995: The representation of the macroscopic behavior of observed moist convective processes. Ph.D. thesis, University of California, Los Angeles, 227 pp.

Lord, S. J., 1982: Interaction of a cumulus cloud ensemble with the large-scale environment. Part III: Semi-prognostic test of the Arakawa–Schubert cumulus parameterization. *J. Atmos. Sci.*, **39,** 88–103.

——, W. C. Chao, and A. Arakawa, 1982: Interaction of a cumulus cloud ensemble with the large-scale environment. Part IV: The discrete model. *J. Atmos. Sci.*, **39,** 104–113.

Lorenz, E. N., 1978: Available energy and the maintenance of a moist circulation. *Tellus,* **30,** 15–31.

——, 1979: Numerical evaluation of moist available energy. *Tellus,* **31,** 230–235.

Manabe, S., J. Smagorinsky, and R. F. Strickler, 1965: Simulated climatology of a general circulation model with a hydrological cycle. *Mon. Wea. Rev.,* **93,** 769–798.

Miyakoda, K., J. Smagorinsky, and R. F. Strickler, and G. D. Hembree, 1969: Experimental extended predictions with a nine-level hemispheric model. *Mon. Wea. Rev.,* **97,** 1–76.

Moorthi, S., and M. J. Suarez, 1992: Relaxed Arakawa–Schubert: A parameterization of moist convection for general circulation models. *Mon. Wea. Rev.,* **120,** 978–1002.

Nicholls, S., and M. A. LeMone, 1980: The fair weather boundary layer in GATE: The relationship of subcloud fluxes and structure to the distribution and enhancement of cumulus clouds. *J. Atmos. Sci.,* **37,** 2051–2067.

Nitta, T., 1975: Observational determination of cloud mass flux distributions. *J. Atmos. Sci.,* **32,** 73–91.

——, 1977: Response of cumulus updraft and downdraft to GATE A/B-scale motion systems. *J. Atmos. Sci.,* **34,** 1163–1186.

——, 1978: A diagnostic study of interaction of cumulus updrafts and downdrafts with large-scale motions in GATE. *J. Meteor. Soc. Japan,* **56,** 232–241.

Ooyama, K., 1971: A theory on parameterization of cumulus convection. *J. Meteor. Soc. Japan,* **49,** 744–756.

Pan, D.-Z., 1995: Development and application of a prognostic cumulus parameterization. Ph.D. dissertation, Colorado State University, 207 pp.

Randall, D. A., and J. Wang, 1992: The moist available energy of a conditionally unstable atmosphere. *J. Atmos. Sci.,* **49,** 240–255.

——, and D.-M. Pan, 1993: Implementation of the Arakawa–Schubert cumulus parameterization with a prognostic closure. *The Representation of Cumulus Convection in Numerical Models,* K. A. Emanuel and D. J. Raymond, Eds., Amer. Meteor. Soc., 137–144.

Sui, C.-H., M.-D. Cheng, X. Wu, and M. Yanai, 1989: Cumulus ensemble effects on the large-scale vorticity and momentum fields of GATE. Part II: Parameterization. *J. Atmos. Sci.,* **46,** 1609–1629.

Thompson, R. M., S. W. Payne, E. E. Recker, and R. J. Reed, 1979: Structure and properties of synoptic scale wave disturbances in the intertropical convergence zone of the eastern Atlantic. *J. Atmos. Sci.,* **36,** 53–72.

Wang, J., 1994: Generalized convective available potential energy (GCAPE) and its application to cumulus parameterization. Ph.D. dissertation, Colorado State University, 215 pp.

——, and D. A. Randall, 1994: The moist available energy of a conditionally unstable atmosphere. Part II: Further analysis of GATE Data. *J. Atmos. Sci.,* **51,** 703–710.

Wu, X., 1993: Effects of cumulus ensemble and mesoscale stratiform clouds in midlatitude convective systems. *J. Atmos Sci.,* **50,** 2496–2518.

Xu, K.-M., and A. Arakawa, 1992: Semi-prognostic tests of the Arakawa–Schubert cumulus parameterization using simulated data. *J. Atmos. Sci.,* **49,** 2421–2436.

——, ——, and S. K. Krueger, 1992: The macroscopic behavior of cumulus ensembles simulated by a cumulus ensemble model. *J. Atmos. Sci.,* **49,** 2402–2420.

Yanai, M., S. K. Esbensen, and J.-H. Chu, 1973: Determination of bulk properties of tropical cloud clusters from large-scale heat and moisture budgets. *J. Atmos. Sci.,* **30,** 611–627.

——, J.-H. Chu, and T. E. Stark, 1976: Response of deep and shallow tropical maritime cumuli to large-scale processes. *J. Atmos. Sci.,* **33,** 976–991.

Zipser, E. J., 1977: Mesoscale and convective-scale downdrafts as distinct components of squall line structure. *Mon. Wea. Rev.,* **105,** 1568–1589.